Electric Power Systems Research 128 (2015) 19–29

Contents lists available at ScienceDirect

Electric Power Systems Research

journal homepage: www.elsevier.com/locate/epsr

Real-time charging coordination of plug-in electric vehicles based on hybrid fuzzy discrete particle swarm optimization

Somayeh Hajforoosh*, Mohammad A.S. Masoum, Syed M. Islam

Department of Electrical and Computer Engineering, Curtin University of Technology, Perth, WA, Australia

ARTICLE INFO

Article history:
Received 16 March 2015
Received in revised form 19 June 2015
Accepted 22 June 2015
Available online 7 July 2015

Keywords:
Plug-in electric vehicles
Online PEV coordination
GA
DPSO
Fuzzy and smart grid

ABSTRACT

The main impact of uncoordinated plug-in electric vehicle (PEV) charging is adding new time-variant loads that can increase the strains on the generation units, transmission and distribution systems that may result in unacceptable voltage drops and poor power quality. This paper proposes two dynamic online approaches for coordination of PEV charging based on fuzzy genetic algorithm (FGA) and fuzzy discrete particle swarm optimization (FDPSO). The algorithms will minimize the costs associated with energy generation and grid losses while also maximizing the delivered power to PEVs considering distribution transformer loading, voltage regulation limits, initial and final battery state of charges (SOCs) based on consumers' preferences. The second algorithm relies on the quality and speed of DPSO solution for more accurate and faster online coordination of PEVs while also exploiting fuzzy reasoning for shifting charging demands to off-peak hours for a further reduction in overall cost and transformer loading. Simulation results for uncoordinated, DPSO, FGA and FDPSO coordinated charging are presented and compared for a 449-node network populated with PEVs. Results are also compared with the previously published PEV coordinated charging based on maximum sensitivity selections (MSS). Main contributions are formulating the PEVs charging coordination problem and applying different optimization methods including online FGA and FDPSO considering different driving patterns, battery sizes and charging rates, as well as initial SOCs and requested final SOCs.

1. Introduction

Recent developments in smart grid (SG) technology along with the growing concerns about the environment have increased the interests of public and electric utilities in PEVs. These vehicles can be beneficial and cost effective to both the consumers and electric utilities if their charging activities are properly coordinated [1]. However, recent studies show that uncoordinated PEV charging can increase the stress on power system, cause voltage drops and rebound peaks [6,31–34]. In general, PEV charging can be performed using centralized [2,3,7–12] and/or decentralized coordination approaches [4,5,13–15].

There are various decentralized methods for PEV charging based on electricity auction [4,13], dual tariffs for PEV owners in several utility service regions [14], and energy cost sharing model [21]. The aim is without relying on a central control unit, each PEV owner be motivated to autonomously adjust its own charging power in response to a communal virtual price signal and its own preferences. However, the outcome of a decentralized approach may or may not be optimal, depending on the information and methods used to determine local charging patterns [22,30]. For instance, dual tariffs are only suitable for the scenario when the market share of PEVs is low [14]. In addition, in decentralized strategies, the network operator uses price incentives to motivate shifting of charging tasks to valleys of the load profile while each PEV owner is responsible for its own charging pattern.

There are also several studies on centralized PEV coordination with various objectives such as valley filling [7], PEV coordination with CHP (combined heat and power) [8] and minimizing distribution feeder losses [3] as well as minimizing the costs associated with energy generation and grid losses [11]. In a centralized PEV coordination strategies, the utility is responsible to coordinate vehicle charging by directly considering grid performance improvements (grid losses and node voltage profiles) while also indirectly looking after PEV owners' benefits by postponing vehicle charging to off-peak hours with inexpensive electricity prices. An aggregator usually makes decisions about the time and rate of all PEV charging in order to achieve near optimal solutions [16]. In addition, the aggregator acts as an interface between customers (PEVs) and the

* Corresponding author. Tel.: +61 411865898.
E-mail addresses: Somayeh.hajforoosh@postgrad.curtin.edu.au (S. Hajforoosh), m.masoum@curtin.edu.au (M.A.S. Masoum), s.islam@curtin.edu.au (S.M. Islam).

http://dx.doi.org/10.1016/j.epsr.2015.06.019
0378-7796/

grid operator and provides charging services considering benefits of both sides [17–20]. In [10,23], PEVs are assumed to have the same battery sizes and chargers while [10] only considers a static charging scenario. In [11] optimal PEV charging is performed using a maximum sensitivity selections (MSS) based algorithm considering the same battery size, charge rates and SOCs for all PEVs. The 34-node small smart grid test system used in [3] for charging of PEVs in a static state.

Although the above-mentioned studies have examined various aspects of the PEV charging coordination, it is imperative to propose an online centralized and comprehensive algorithm that is applicable to power market with time-varying market energy prices (MEP) considering the charging demand based on customers' behavior for each PEV with different battery sizes and charger types. Furthermore, for online applications, the speed and computing time of the coordination algorithm plays a vital role, as the aggregator will execute it at each timeslot with updated load profiles in order to obtain a new charging schedule.

In this paper two dynamic heuristic based approaches based on hybrid (FGA) and hybrid (FDPSO) optimization are proposed for online charging of PEV batteries in SG. The algorithms minimize the cost associated with energy generation and grid losses while also maximizing the delivered power to PEVs, regulating node voltages and reducing distribution transformer loading. Simulations results for a 449-node SG network are presented and compared with online coordinated PEV charging using MSS [11], GA, DPSO, FGA and FDPSO approaches.

2. Problem formulation

Online coordination of PEV charging is a dynamic and real time optimization problem that requires formulation of a comprehensive objective function and a high-speed optimization method to capture near-optimal solutions. In this paper, the optimization variable is the charging status of PEVs, where charging rate is variable for different PEV types. However, during the charging progress it is considered that charging rate is constant. The nonlinear objective function of Eq. (1) is defined for the PEV coordination problem to maximize the delivered charging power ($F_{DCP}(t)$) to PEVs at each timeslot ($\Delta t = 5$ min), while the costs associated with energy generation ($F_{cost\text{-}gen}(t)$), and grid losses ($F_{cost\text{-}loss}(t)$) are also minimized:

$$Max \quad F(t) = \frac{F_{DCP}(t)}{F_{\cos t-loss}(t) + F_{\cos t-gen}(t)} = \frac{\sum_{i=1}^{N_{PEV}} (\text{Delivered charging power}(i,t))}{\sum_t K_E P_{loss}(t) + \sum_t K_{t,G} D_{total}(t)} \quad \text{for} t = \Delta t, 2\Delta t, \ldots, 24\,\text{h} \tag{1}$$

where $P_{loss}(t) = \sum_{k=0}^{n-1} R_{k,k+1}(|V_{k+1}(t) - V_k(t)||y_{k,k+1}|)^2$, K_E and $K_{t,G}$ are the costs per MWh of losses [11,12] and generation (Fig. 3(b)), respectively; $\Delta t = 5$ min is the timeslot; k and n are the node number and total number of nodes; $R_{k,k+1}$ and $y_{k,k+1}$ are the resistance and reactance of the line segment between nodes k and $k+1$, respectively.

Eq. (1) is subject to the following voltage (Eq. (2)), demand for each timeslot (Eq. (3)), and SOC constraints (Eq. (4)) to preserve power quality and supplying the base and PEV loads.

$$V_{\min} \le V_k(t) \le V_{\max}, \quad \text{for} \quad k = 1, \ldots, n \tag{2}$$

$$D_{total}(t) = \sum_{k=1}^{n} P_k(t) = \sum_{k=1}^{n} (P_{Load_K}(t) + P_{PEV_K} \le D_{\max}(t)) \quad t = \Delta t, 2\Delta t, \ldots. \tag{3}$$

where $D_{\max}(t) = Max\{DL(\Delta t), DL(2\Delta t), \ldots, DL(m\Delta t)\}$, $m = 1, \ldots, 288$

$$SOC(i,t) \le SOC_{Req}(i) \le SOC_{\max}, i = 1, \ldots, N_{PEV} \tag{4}$$

where V_{min} and V_{max} are the lower and upper voltage limits, respectively; $D_{max}(t)$ is the maximum demand level that would normally occur without any PEVs during a day. In this paper, $D_{max}(t)$ is selected to be 0.84 MW corresponding to the maximum load for the selected DLC. $SOC(i,t)$ is the SOC for the ith PEV at t, $SOC_{Req}(i)$ is the requested SOC for the ith PEV, $SOC_{\max}$ is the state of charge of each battery when the battery is fully charged, P_{Loadk} is the base-load power, DL is the daily load at mth timeslot, and P_{PEVk} is the consumed power for the PEV at node k.

In this paper, $SOC_{initial}$ at plug-in time is driven from driving pattern for each PEV [29]:

$$F(t) = \begin{cases} \alpha_i - (\alpha_i - \beta_i) \times \frac{L_j}{L_i^{\max}} & L_j \le L_i^{\max} \\ \beta_i & \text{otherwise} \end{cases} \quad \text{for} \quad i = 1, 2, 3, \quad j = 1, \ldots\ldots, N_{PEV} \tag{5}$$

where i indicates the type of PEVs, j is number of PEVs, L_j is the trip path for jth PEV, and $L_i^{\max}$ is the rated length path that each type of PEVs can trip [29]. In this paper, the selected values for parameters α_1, α_2 and α_3 are 0.85, 0.8, and 0.75, β_1, β_2 and β_3 are 0.15, 0.2 and 0.25; and L_1, L_2 and L_3 are 40, 50, 60 miles, respectively. In addition, three types of PEVs including e-Golf (Type 1), Honda Fit (Type 2), Ford C-Max (Type 3) with chargers' rates of 7.2, 6.6, 3.3 kW and corresponding battery sizes of 24, 20, 7.6 kWh (with 88% efficiency) are considered [28].

It is also assumed that aggregator has access to PEV information using smart metering technology to monitor their locations, charger types, battery sizes, initial and requested SOCs ($SOC_{initial}$ and SOC_{Req}). The scheduling horizon starts at 16:00 h for 24-h, and is divided into 288 timeslots of $\Delta t = 5$ min. As a result, after plugging a new PEV at Δt, the grid loads will be updated and the proposed coordination algorithm will be executed to obtain a new optimal charging schedule. In addition, in this paper no constraint is assumed for the charging time and vehicles might be plugged-in at any time during the 24-h time horizon. However, if vehicles are plugged-out before the designated departure time (next day at 6am) then they may not be fully charged.

In this paper, the backward-forward sweep method is used to calculate load flows and bus voltages [3], and it is considered that the generation capacity is large enough to supply both base and charging load in all timeslots. It should be noted that if a PEV owner prefer to charge without being schedulable, the PEV will be part of the base load. As the optimization is real-time, changing the base load does not affect on the optimization results.

3. Proposed online heuristic based coordination algorithms for PEV charging

Many practical problems including optimal PEV coordination have discrete nature; therefore, two PEV charging approaches incorporating fuzzy reasoning based on DPSO [25] and binary genetic algorithm are developed to solve Eqs. (1)–(4).

3.1. DPSO formulation

The discrete version of PSO is very similar to the original continuous algorithm except for the state equations listed below (Eqs. (6)–(8)). In DPSO formulation, the position and velocity of each particle are vectors in the d-dimensional binary solution space $x_i \in \{0 \quad 1\}^d$ and the continuous space, respectively. The

probability of an agent making a decision (e.g., yes or no, true or false) is a function of the personal and social factors [26]:

$$P(X_{pt,j}^{it+1} = 1) = f(X_{pt,j}^{it}, V_{pt,j}^{it}, pbest_{pt,j}, gbest_j) \quad (6)$$

where $X_{pt,j}^{it}$ is the location of the particle pt in generation it, $pbest_{pt,j}$ is the best point found by particle pt in its past life up to the current generation, $gbest_j$ is the best overall point found by the swarm of particles in their past life and $V_{pt,j}^{it}$ is the agent's alternative choice tendency that determines a probability threshold in the range of [0,1]. For example, higher and lower values of $V_{pt,j}^{it}$ indicate that the agent is more likely to favor 1 and 0 choices, respectively. A sigmoid function can be used to accomplish this threshold:

$$sig(V_{pt,j}^{it}) = \frac{1}{1 + \exp(-V_{pt,j}^{it})} \quad (7)$$

In a manner similar to construction of the conventional continuous PSO, formulation of DPSO is described as [18]:

$$V_{pt,j}^{it+1} = V_{pt,j}^{it} + rand_1(pbest_{pt,j} - X_{pt,j}^{it}) + rand_2(gbest_j - X_{pt,j}^{it}) \quad (8a)$$

$$\text{if} \quad \rho_{pt,j}^{it+1} < sig(V_{pt,j}^{it}) \quad \text{then} \quad X_{pt,j}^{it+1} = 1, \quad \text{else} \quad X_{pt,j}^{it+1} = 0 \quad (8b)$$

where $rand_1$ and $rand_2$ are positive random numbers generated from a uniform distribution [25,26] with a predefined upper limit while $\rho_{pt,j}^{it+1}$ is a random number between 0 and 1.

Eqs. (6)–(8) are used in an iterative procedure over each j dimension of each particle to arrive at a near-global solution. The maximum value of $V_{pt,j}^{it}$ is often limited to [−4, +4] to ensure that $sig(V_{pt,j}^{it})$ will not get too close to the interval limits [0,1].

3.2. DPSO initial population and structure of particles

In the selected initial population structure, each particle (chromosome) contains the status of all PEVs where digit "1" corresponds to a PEV being charged while digit "0" indicates the charging has not been started or already finished. Initial population structure is:

$$\text{Number of population} \begin{pmatrix} Status_{PEV\,1} & Status_{PEV\,2} & \cdots & Status_{PEV\,n} \\ Status_{PEV\,1} & Status_{PEV\,2} & \cdots & Status_{PEV\,n} \\ \vdots & \vdots & \vdots & \vdots \\ Status_{PEV\,1} & Status_{PEV\,2} & \cdots & Status_{PEV\,n} \end{pmatrix} \quad \text{Number of PEVs} \quad (9)$$

3.3. DPSO fitness function

To improve the quality of DPSO solution and achieve further cost reduction, fuzzy fitness functions are used for the objective and constraints (Eqs. (1)–(4)). The inverse algebraic product (Eq. (10)) of the proposed penalty functions for voltage (Eqs. (11) and (12)) and demand (Eq. (13)) is used as the fitness function to combine the PEV coordination objective function (Eq. (1)) and constraints (Eqs. (2)–(4)):

$$F_{fitness}(t) = \frac{F(t)}{F_V(t) \times F_D(t)} \quad (10)$$

$$F_V(t) = \prod_{k=1}^{n} F_{V,k}(t) \quad (11)$$

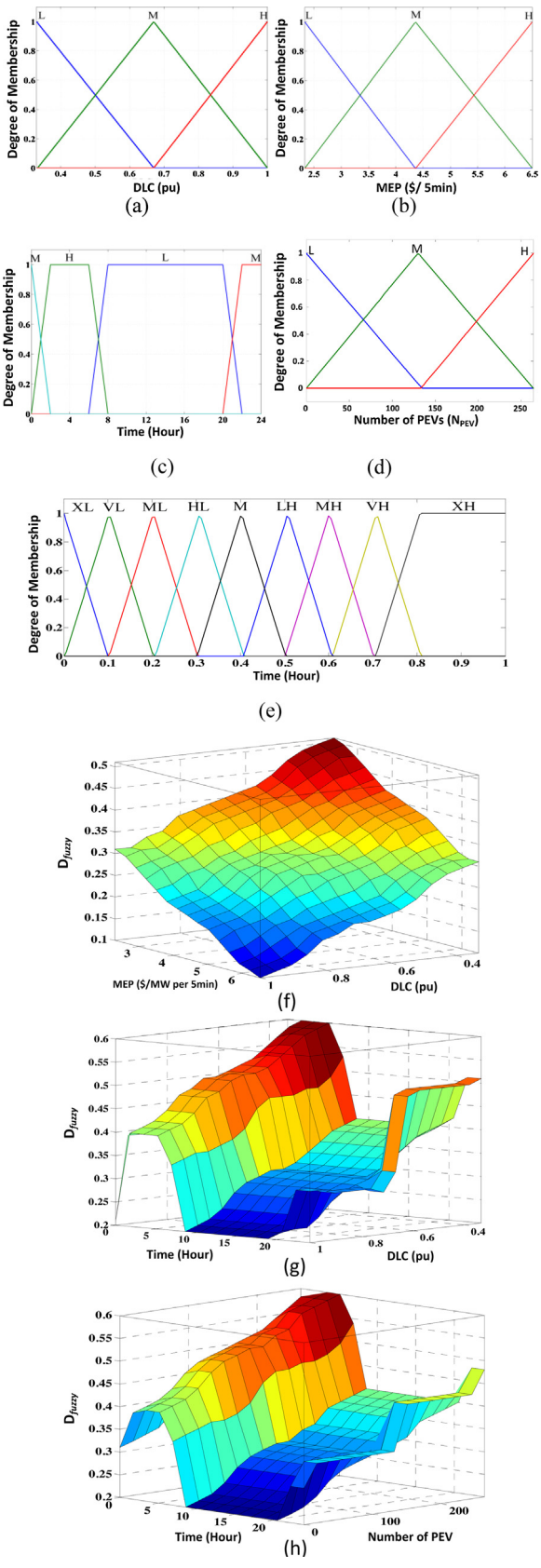

Fig. 1. Proposed FES membership functions for: (a)–(e) the three-level inputs DLC, MEP (Fig. 3(b)), time and Npev, (e) the nine-level output of D_{fuzzy}, fuzzy surfaces for $D_{fuzzy}(t)$ variations based on; (f) DLC and MEP, (g) DLC and time, (h) Number of PEV and time.

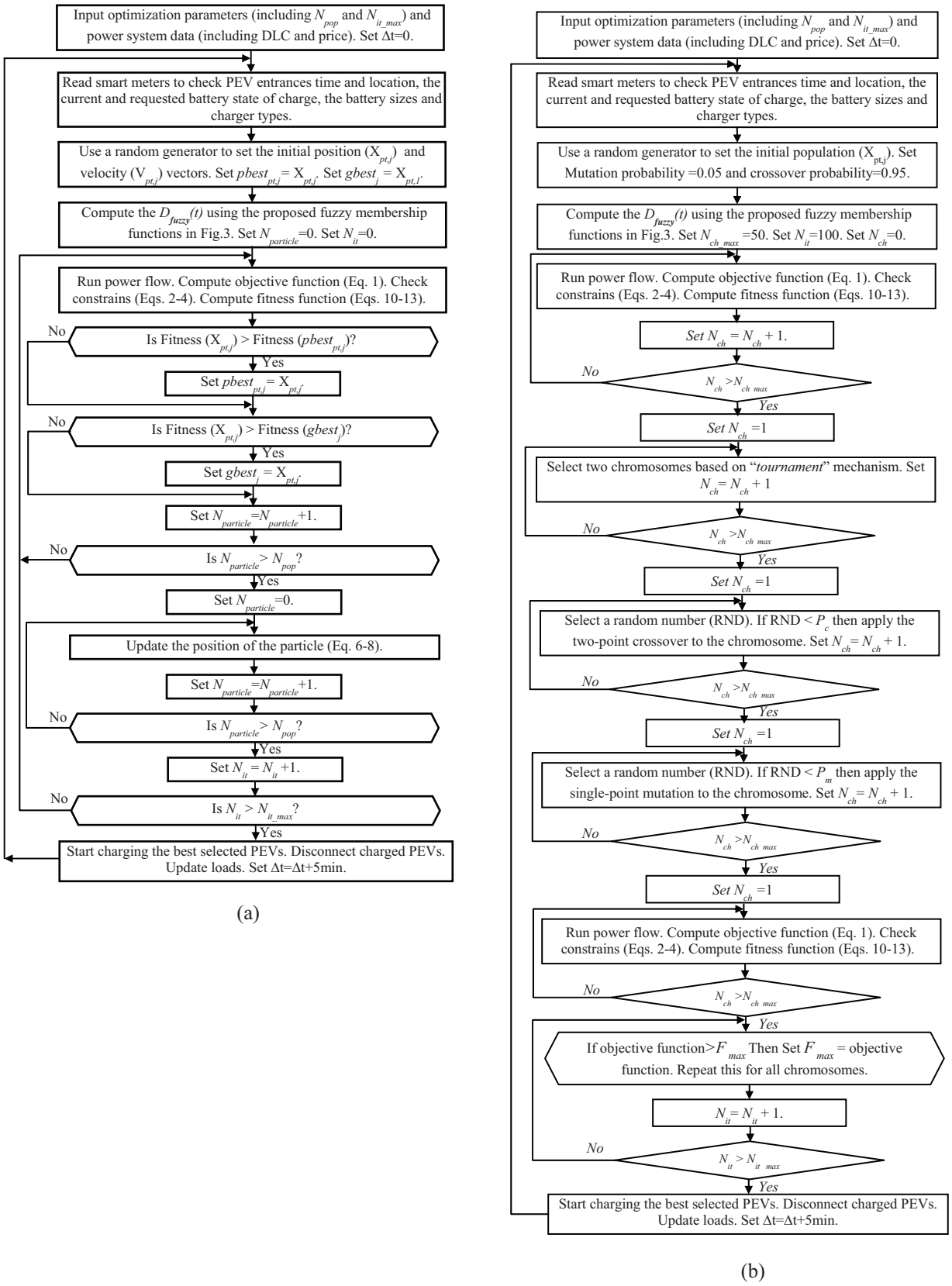

Fig. 2. Flow charts of the proposed algorithms for the online PEV charging coordination, (a) FDPSO, (b) FGA.

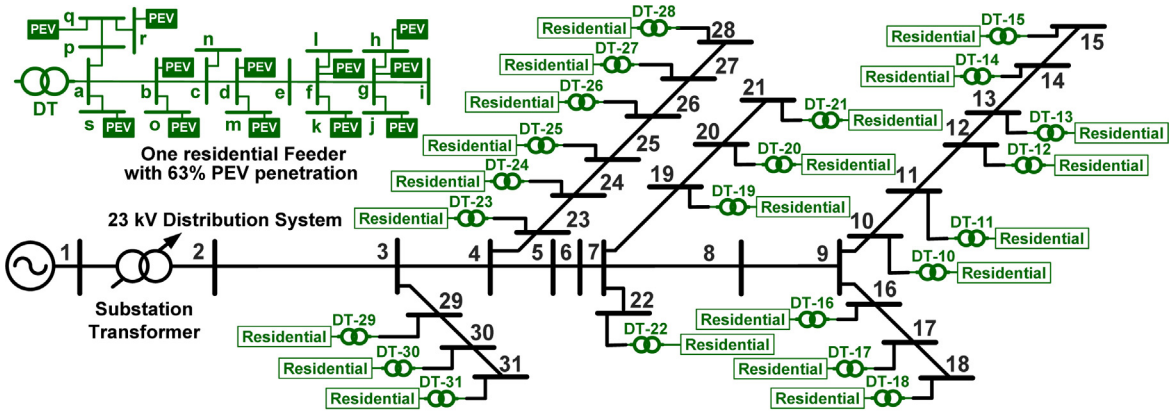

(a)

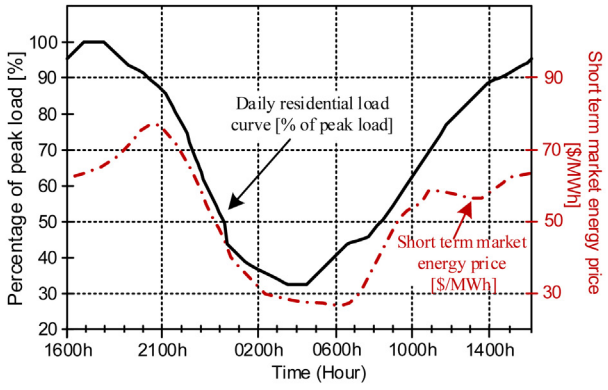

(b)

Fig. 3. (a) The 449-node smart grid consisting of IEEE 31-node 23 kV system and 22 low voltage 19-node 415 V residential feeders populated with PEVs [11], (b) daily residential load curve (DLC) and short term market energy price (MEP) [11,12].

$$F_{V,k}(t) = \begin{cases} e^{\alpha_{V_1}(1-V_k(t))} & V_k(t) \le V_{\min} \\ 1 & V_{\min} \le V_k(t) \le V_{\max} \\ e^{\alpha_{V_2}(V_k(t)-1)} & V_k(t) \ge V_{\max} \end{cases} \quad (12)$$

$$F_D(t) = \begin{cases} 1, & D_{total}(t) \le D_{fuzzy}(t) \\ e^{\alpha_D(D_{total}(t)-D_{fuzzy}(t))}, & D_{total}(t) \ge D_{fuzzy}(t) \end{cases} \quad (13)$$

where $F(t)$, $F_V(t)$ and $F_D(t)$ are the penalty functions, bus voltage penalty function and demand (distribution transformer loading) penalty function at each timeslot, respectively. $D_{fuzzy}(t)$ is the adjusted maximum demand level ($D_{max}(t)$) at each timeslot which is determined by the fuzzy surfaces and membership functions of Fig. 1; α_{V1}, α_{V2} and α_D are the coefficients used to adjust the slopes of the penalty functions.

3.4. Fuzzy expert system (FES) for adjusting maximum demand

For a further reduction in the generation cost $F_{cost\text{-}gen}(t)$ (Eq. (1)), the maximum demand level $D_{max}(t)$ (Eq. (3)) is first adjusted at each timeslot (e.g., $D_{fuzzy}(t)$ = adjusted $D_{max}(t)$) using the fuzzy expert system (FES) of Fig. 1 and then used to calculate the demand penalty function of Eq. (13). The proposed FES of Fig. 1(a)–(e) consists of three-level (low (L), medium (M) and high (H)) input membership functions for daily load curve (DLC) (Fig. 3(b)), market energy price (MEP) (Fig. 3(b)), time, and Npev as well as a nine-level (extreme low (XL), very low (VL), medium low (ML), high low (HL), medium (M), low high (LH), medium high (MH)), very high (VH) and extreme high (XH)) output membership function for $D_{fuzzy}(t)$. Therefore, FES considers the impacts of DLC, time, MEP and Npev to dynamically adjust $D_{fuzzy}(t)$ at each timeslot. This is more clearly demonstrated using the fuzzy surfaces of Fig. 1(f)–(h) that illustrate $D_{fuzzy}(t)$ variations based on DLC-Npev, DLC-time, and Npev-time respectively. For example, less PEV charging is performed by assigning low membership functions to $D_{fuzzy}(t)$ during the early evening hours when both DLC and MEP are high (Fig. 1(f)). On the other hand, as the time approaches the early morning hours with less chance to fully charge all PEVs, higher membership values are assigned to $D_{fuzzy}(t)$ in order to quickly charge the vehicles and also take advantage of the low energy prices (Fig. 1(f)).

According to Fig. 1(h), an increase in the number of PEVs during on-peak hours will force the aggregator to charge more PEVs in order to prevent undesired overloading conditions at later hours. The results of this paper indicated that the proposed fuzzy method will result in reduce of the total charging cost for 24-h. In reality, based on the market energy price and DLC as well the available time to charge PEVs, the aggregator needs to adjust the generation curve such that the total cost for 24-h is minimized.

3.5. Flow chart of proposed FDPSO algorithm

Fig. 2(a) shows the flow chart of the proposed FDPSO algorithm for optimal online PEV charging based on Eqs. (1)–(4) and (10)–(13) and Fig. 1. In this figure, N_{pop} and N_{it} represent PSO population size and number of iterations, respectively.

Table 1
PEV charging scenarios for the SG system of Fig. 3(a).

Case	Online charging approach	Simulations
A	Uncoordinated	Figs. 4 and 8, Table 2
B	MSS coordinated [11]	Table 2
C	DPSO coordinated: (Fig. 2(a) without fuzzification)	Figs. 5 and 8, Table 2
D	FDPSO coordinated (Fig. 2(a))	Figs. 6 and 8, Table 2
E	GA coordinated (Fig. 2(b) without fuzzification and replacing DPSO with GA)	Table 2, Fig. 8
F	FGA coordinated (Fig. 2(b))	Table 2, Figs. 7 and 8

3.6. Proposed hybrid fuzzy genetic algorithm (FGA)

To investigate the performance, quality and speed of the proposed online FDPSO PEV coordination algorithm, a new hybrid fuzzy genetic algorithm (FGA) based on Fig. 1 is also implemented. In this paper, the algorithm uses two-point crossover, non-uniform mutation and tournament selection methods [24,27] with selected crossover and mutation probabilities of 0.9 and 0.05, respectively. Fig. 2(b) shows the flow chart of the proposed FGA algorithm for optimal online PEV charging based on Eqs. (1)–(4) and (10)–(13).

4. The 449-node smart grid test system

The test system of Fig. 3(a) is used to evaluate the performance and accuracy of the proposed FDPSO and FGA methods. It includes the IEEE 31-bus 23 kV distribution network connected to 22 low voltage 415 V residential feeders. Each residential feeder consists of 19 nodes representing customer households. System data including lines and residential loads' parameters are available in [11].

5. Simulation results

Simulations are performed on SG of Fig. 3(a) for the six case studies of Table 1 for each timeslot, $\alpha_{V1} = \alpha_{V2} = 0$, $\alpha_D = 0.5$ (Eqs. (12) and (13)) and PEV penetration levels of 0% (e.g., no PEVs), 16% (67-PEV), 32% (134-PEV), 47% (197-PEV) and 63% (264-PEV). In addition, two more scenarios with 3 and 5 percent of PEVs penetrations are shown for cases A and D. Moreover, there are 30% of PEV type 1, 40% of PEV type 2, and 30% of PEV type 3.

5.1. Case A: uncoordinated PEV charging

The impact of uncoordinated PEV charging is investigated by starting the charging process as soon as vehicles are randomly plugged-in. Detailed simulation results including daily generation cost, total system losses and system power consumption are presented in Fig. 4 and summarized in Table 2 (rows 4–10). Daily generation cost can be obtained using Eq. (14).

$$\text{Daily generation cost} = \sum_{m=1}^{288} \text{Generation cost}(m\Delta t) \tag{14}$$

As expected, the SG is facing overloading, voltage regulation and efficiency problems.

For example, for 63% PEV penetration, maximum power consumption, maximum system losses and cost have increased by about 42% (Fig. 4(a)), 157% (Fig. 4(b)) and 69% (Fig. 4(c)), respectively; compared to the nominal operation with no vehicles.

5.2. Case B: online MSS based PEV charging algorithm

The online MSS based PEV charging algorithm of [11,12] quantifies the objective function sensitivities to PEV charger loads in the smart grid at a given time step. This is achieved by temporarily activating all PEVs in the queue at the current time step (at 5% of their nominal power rating). From the small load power perturbations at each PEV charger node, it is then possible to conveniently compute the sensitivities of system losses due to each of the candidate PEV nodes from Jacobian entries of the load flow, which is then stored in the MSS vector. The MSS vector is then sorted such that PEVs contributing to the highest loss sensitivities in each priority group are selected last. In this manner, the PEV coordination solution is designed to favor scheduling first the PEVs causing minimum impact on system losses. This MSS sorting process is repeated for descending priority groups thereby arriving at a sorted PEV queue table in accordance with the MSS vector.

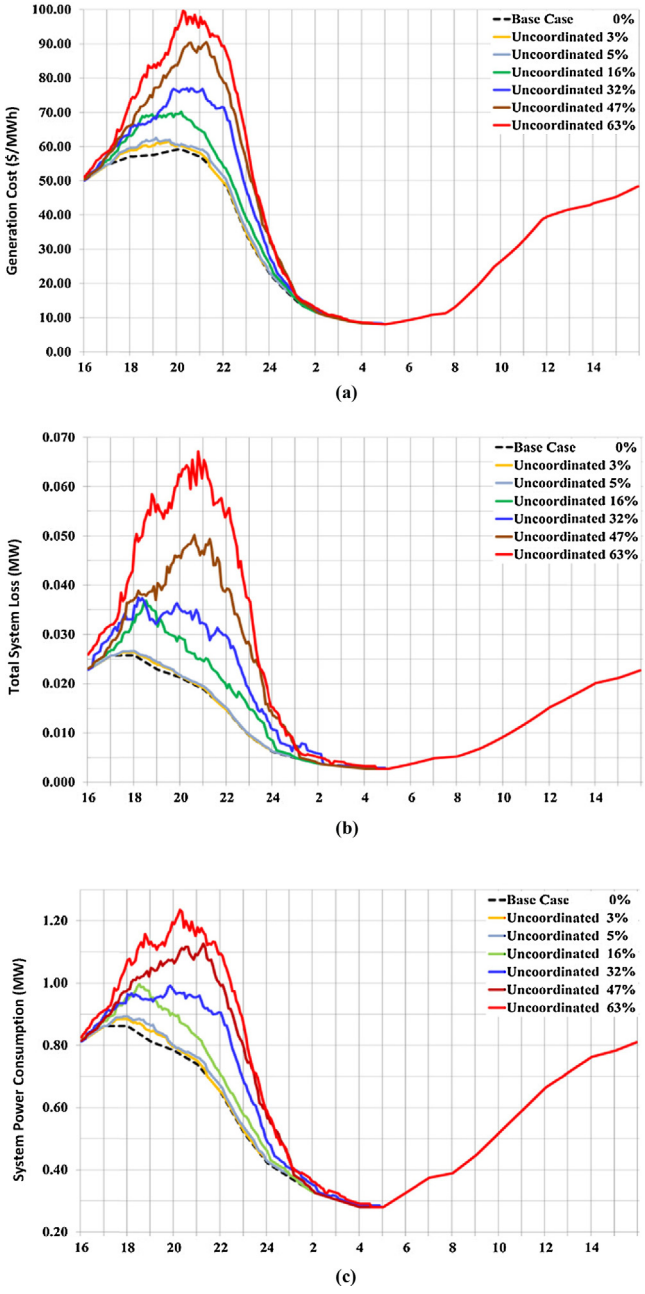

Fig. 4. Case A (Table 1): simulation results for SG of Fig. 3; (a) generation cost, (b) total system losses, (c) system power consumption.

Table 2
Impact of (un)coordinated PEV charging on the SG of Fig. 3(a).

PEV [%]	ΔV [%]*	I_{MAX} [%]**	Total generation cost [$/day]	Average generation cost [$/MWh]***	Total cost [$/day]	Increase in total cost [%]	Computing time**** [s]
Nominal case: with no PEV (0% PEV penetration)							
0	7.63	0	761.51	56.02	776.47	0	NA
Case A: uncoordinated PEV charging; Figs. 4 and 8							
3	7.65	2.62	770.40	56.22	785.51	1.16	NA
5	7.66	3.64	776.59	56.37	791.79	1.97	NA
16	15.11	14.62	827.69	58.20	843.27	8.60	NA
32	17.65	15.03	876.09	59.17	893.60	15.08	NA
47	19.55	30.69	930.60	60.15	951.25	22.51	NA
63	23.40	43.39	978.91	60.95	1004.04	29.31	NA
Case B: comparison between FDPSO (row 12) and MSS (row 13) [11]*****							
63	9.86	0.2	859.66	56.11	879.39	11.70	0.033
63	10.0	0.172	886	57.83	906	15.04	NA
Case C: online DPSO PEV coordination; Figs. 5 and 8							
16	9.32	0.82	826.06	56.43	841.22	8.34	0.026
32	9.38	0.93	867.02	56.86	883.50	13.78	0.028
47	9.90	0.99	900.18	58.12	918.59	18.30	0.031
63	9.90	2.72	902.35	58.60	946.84	21.94	0.032
Case D: online FDPSO PEV coordination; Figs. 6 and 8							
3	7.63	0.11	768.73	56.11	783.82	0.94	0.026
5	7.63	0.12	775.39	56.31	790.55	1.81	0.026
16	8.17	0.65	820.40	56.43	835.30	7.57	0.027
32	8.42	0.67	851.10	56.59	867.52	11.72	0.029
47	9.86	0.99	877.17	56.68	895.25	15.30	0.033
63	9.86	1.70	897.88	56.87	917.55	18.17	0.034
Case E: online GA PEV coordination; Fig. 8							
16	9.88	0.83	826.16	56.83	841.32	8.35	0.045
32	9.90	0.95	866.87	57.64	883.50	13.78	0.047
47	10.00	0.99	900.91	58.21	919.41	18.41	0.050
63	10.00	2.72	928.24	58.79	948.30	22.13	0.052
Case F: online FGA PEV coordination; Figs. 7 and 8							
16	9.90	0.66	820.40	56.43	835.31	7.58	0.047
32	9.90	0.68	851.11	56.59	867.67	11.74	0.048
47	9.90	0.99	877.38	56.69	895.43	15.32	0.052
63	10.0	1.70	901.57	57.10	921.09	18.62	0.054

* Average voltage deviation over 24 h (Eq. (2)).
** Increase in transformer current compared with nominal case (no PEVs).
*** Calculated by dividing "Total generation cost in $/day (column 4)" with "Total daily generation in MWh/day".
**** Intel Core i5-3570 3.40 GHz processor, 8 GB RAM, using MatLab ver. 8.
***** In this case, for each PEV battery size is 8 kW, $SOC_{initial}$ = 0% and SOC_{Req} = 100%.

To compare the results and present the accuracy of the proposed methods, a case study based on using MSS algorithm [11] is investigated when PEVs' penetration is 63%, each PEV battery size is 8 kW, $SOC_{initial}$ = 0% and SOC_{Req} = 100%. The obtained results are compared in Table 2 (rows 12–13) for FDPSO and MSS methods.

5.3. Case C: DPSO coordinated PEV charging

A discrete PSO coordination algorithm without fuzzy reasoning (Fig. 2(a) without any fuzzification) is adopted to improve the system performance. Simulation results are presented in Fig. 5 and Table 2 (rows 14–18). Compared to Case A, DPSO is offering further reduction in transformer overloading (Fig. 5(c)), maximum generation cost level (reduced from 100$/MWh (Fig. 4 (a)) to 69.21$/MWh (Fig. 5(a))) and maximum system losses (reduced from 0.067 MW to 0.034 MW), as well as the total cost (reduced from 1004.04$/MW per day to 946.84$/MW per day). These results show significant improvements in system performance by elegantly shifting period of peak losses from 19:00 h–22:00 h to 24:00 h–2:00 h.

5.4. Case D: FDPSO coordinated PEV charging

The FES of Fig. 1 is included in the DPSO coordination strategy (Fig. 2(a)) to achieve a near-optimal solution with more improvements in system performance. Simulations results are presented in Fig. 6 and Table 2 (rows 19–25).

Compared to Case C, FDPSO is more strictly preventing system (transformer) overloading (Fig. 6(c)) by relying on expert fuzzy reasoning to dynamically adjust (reduce) the maximum power consumption level. For example, for 63% PEV penetration, the maximum power consumption that was 0.88 MW for DPSO algorithm (from 18:30 h to 24:30 h, Fig. 5(c)) is now improved with minimum and maximum values of 0.67 MW and 0.86 MW at 22:55 h and 2:15 h, respectively (Fig. 6(c)).

Note that the impact of time is considered by charging more vehicles during the later morning hours (e.g., 12:300 h–02: 30 h, Fig. 6(c)). This is done by FES to increase the chance of having all vehicles fully charged before 06:00 h for the next day trips.

Comparing Figs. 5 and 6, FDPSO is offering further decreases in maximum generation cost level (from 69.21$/MWh to 63.18$/MWh) and maximum system losses (from 0.034 MW to 0.032 MW) while providing an additional saving in total cost from 946.84$/MW per day to 917.55$/MW per day (Table 2).

5.5. Cases E and F: GA and FGA coordinated PEV charging

For further investigations on the performance and accuracy of the proposed FDPSO, two online PEV coordination strategies based

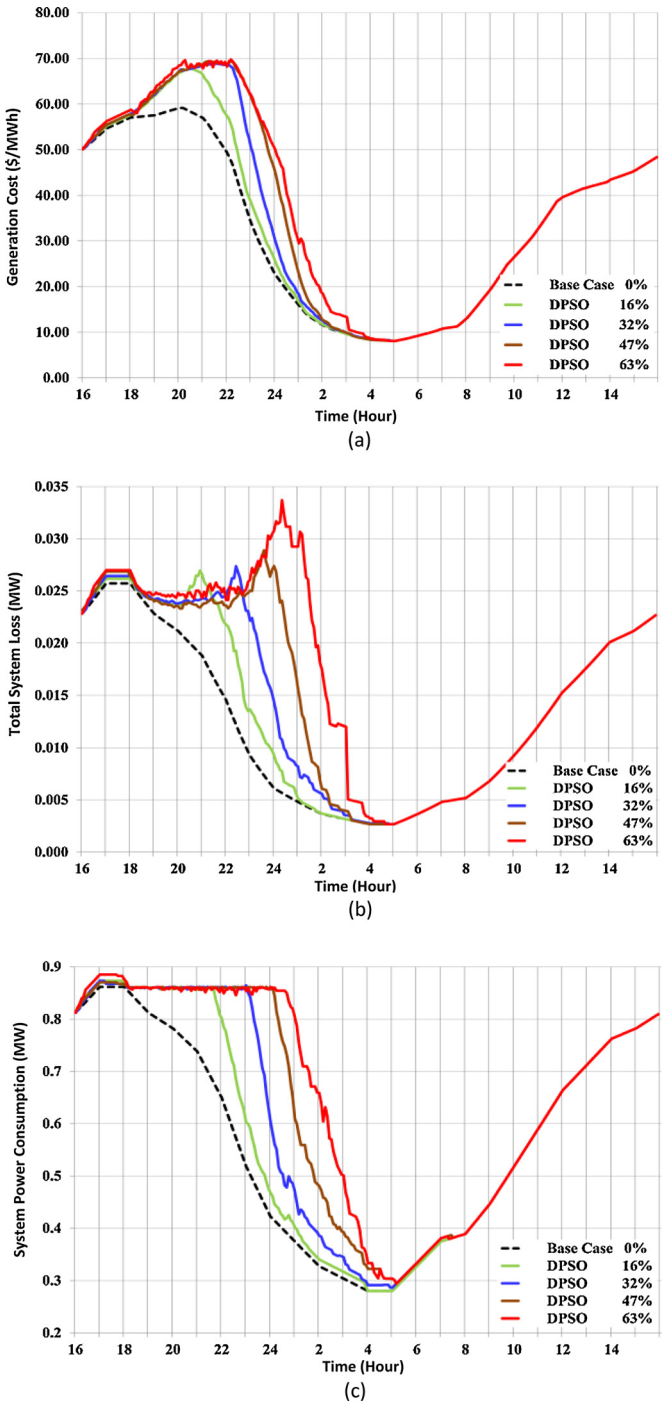

Fig. 5. Case C (Table 1): simulation results for SG of Fig. 3; (a) generation cost, (b) total system losses, (c) system power consumption.

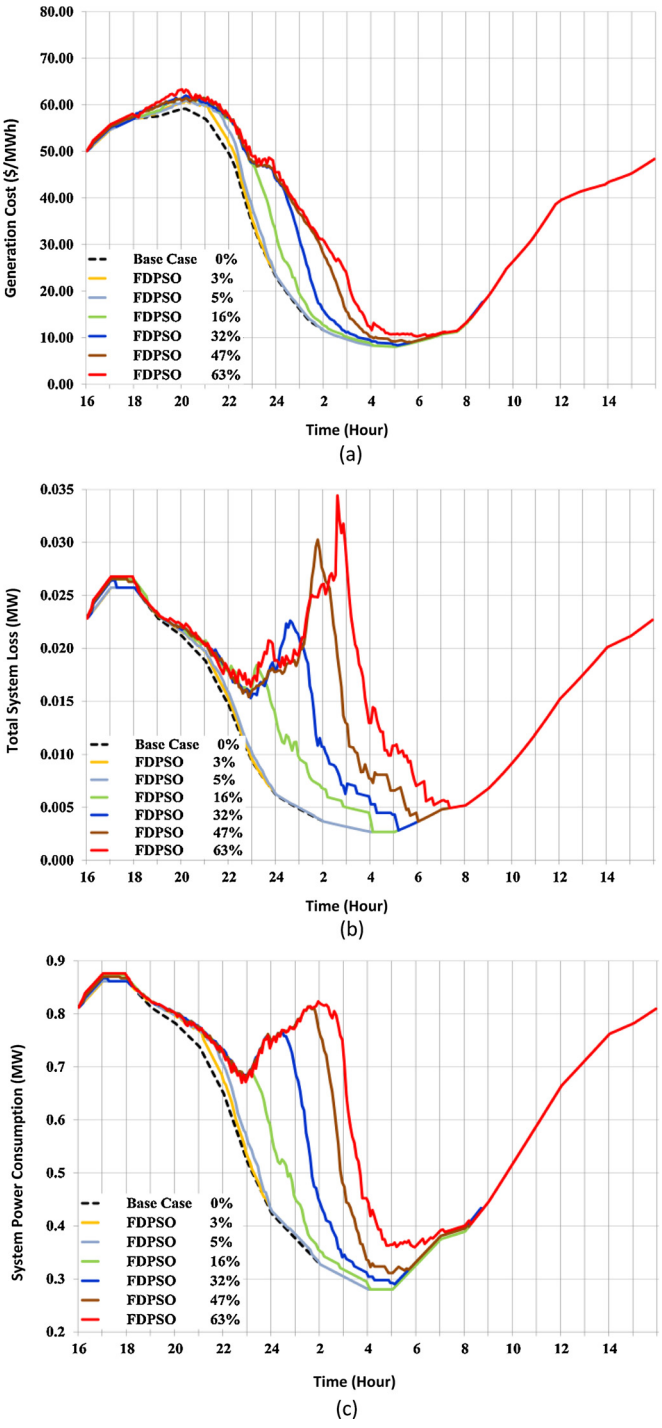

Fig. 6. Case D (Table 1): simulation results for SG of Fig. 3; (a) generation cost, (b) total system losses, (c) system power consumption.

on GA and FGA (Fig. 2(b)) are also developed and tested on the SG network of Fig. 3(a). These algorithms are similar to the DPSO and FDPSO (Fig. 2(a)) with the exception of using binary genetic optimization instead of DPSO. Simulation results (Fig. 7 and Table 2; rows 26–35) are very similar to Cases C and D confirming their accuracy. However, DPSO based approaches are fundamentally faster and more suitable for online applications such as the online PEV coordination problem of this paper (Table 2; last column).

6. Analyses and discussion

6.1. Average and worst node voltage profiles

Fig. 8(a) shows the per unit (pu) system average voltage (AV) and the node worst voltage (WV) profiles within the 24 h for 63% penetration with uncoordinated (Case A) and coordinated (Cases C, D and F) charging schemes.

Note that the weakest node voltage is improved from 0.84 pu (uncoordinated PEV charging) to 0.90 pu for the DPSO, FDPSO and FGA coordinated charging. It is also observed that AVs are improved

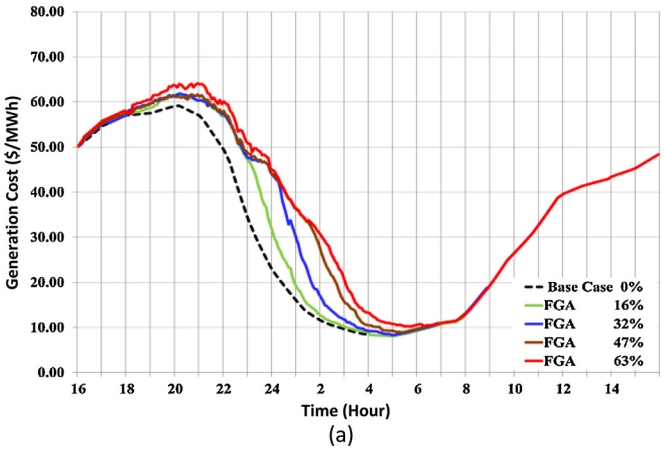

(a)

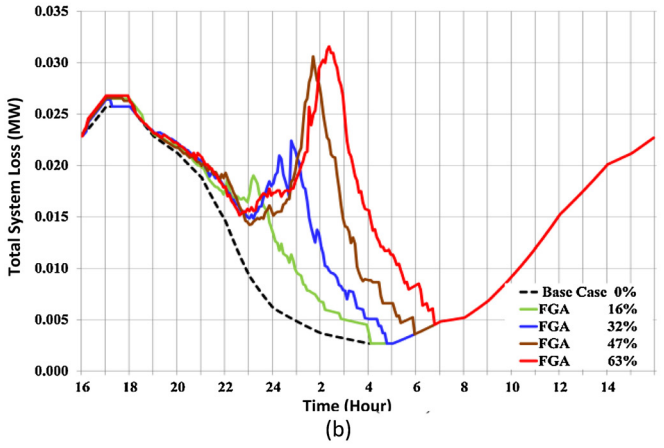

(b)

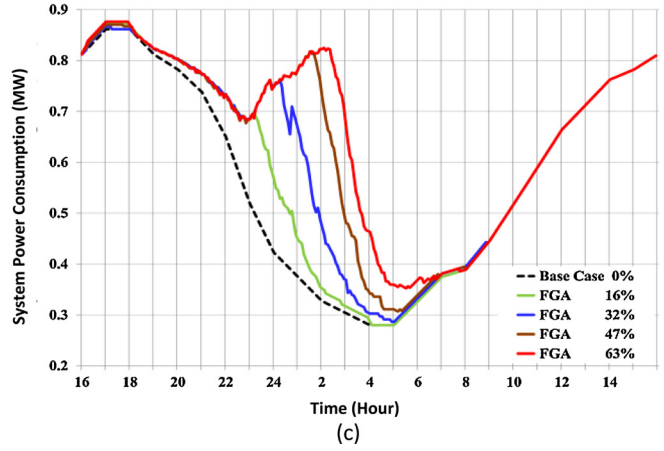

(c)

Fig. 7. Case F (Table 1): simulation results for SG of Fig. 3; (a) generation cost, (b) total system losses, (c) system power consumption.

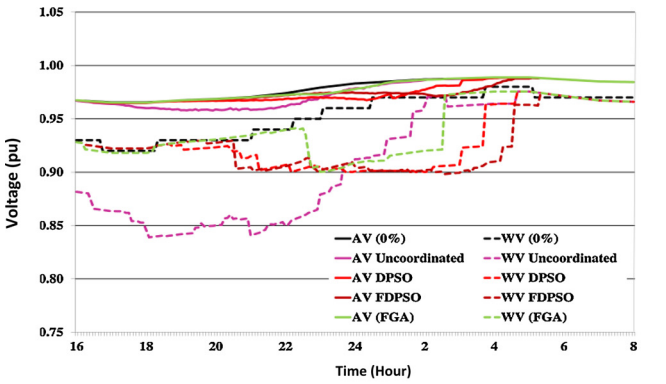

(a)

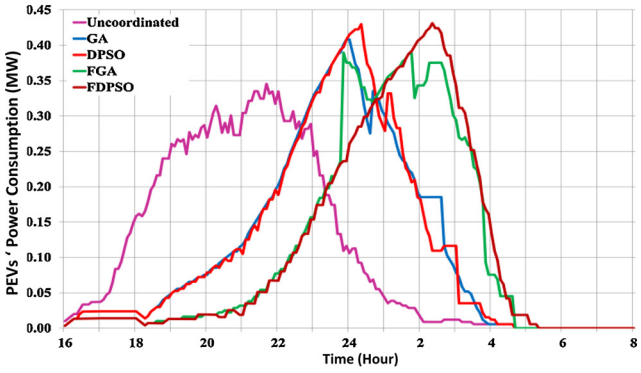

(b)

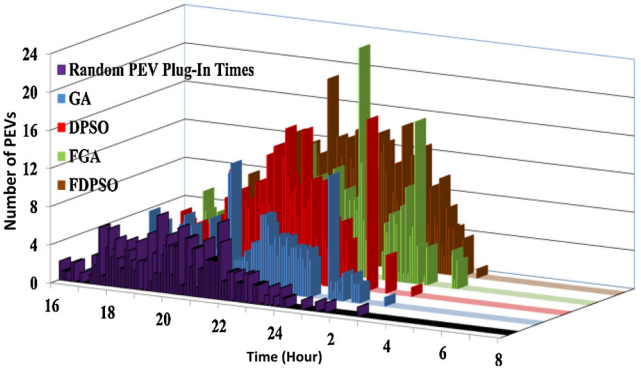

(c)

Fig. 8. (a) System average voltage (AV) and node worst voltage (WV) profiles for Cases A, C, D and F for 63% PEV penetration. (b) Total power consumptions to charge PEVs for Cases A, C, D, E and F with 63% PEV penetration, (c) random plug-in times (Case A) and coordinated charging schedules for Cases C, D, E, and F with 63% PEV penetration.

from 0.96 pu for the case of uncoordinated charging to higher than 0.97 pu when one of the coordinated DPSO, FDPSO or FGA algorithms is used.

6.2. Total power consumption for charging PEVs

Fig. 8(b) compares the power consumption profiles for uncoordinated and coordinated PEV charging. Note that:

The DPSO of Case C postpones vehicle charging activities based on smart meter information using online cost minimization (Eqs. (1)–(4)) at each timeslot of $\Delta t = 5$ min. The peak power consumption time is delayed from around 21:30 h to 24:30 h to reduce system loading during peak load hours while its magnitude is increased from 0.34 MW to 0.43 MW to purchase cheaper energy and reduce $F_{cost\text{-}gen}(t)$. This phenomenon, known as rebound peaks, has been previously noticed and reported in the literature [31–34].

- The FDPSO and FGA-CA strategies of Cases D and F use the additional privileges of the expert knowledge and rely on fuzzy reasoning to achieve better near-optimal solutions that further delays the peak power consumption time to around 02:30 h.
- All coordination algorithms have successfully charged PEVs before 06:00 h. The last vehicle charging is completed at 4:45 h,

04:45 h, 05:30 h and 05:40 h for Cases A, C, D and F, receptively; however, inclusion of FES (Cases D and F) offers more cost savings (Fig. 8, Table 2).

6.3. Random plug-in times and PEV charging schedules

The first row in Fig. 8(c) illustrates the random numbers and random plug-in times of the vehicles for 63% PEV penetration that also corresponds to the uncoordinated vehicle charging schedule of Case A. The remaining four rows show coordinated PEV charging schedules for different coordination methods. As expected, charging patterns for coordinated cases are shifted to off-peak hours.

6.4. Computing times of proposed coordination algorithms

While the quality of the proposed FDPSO and FGA solutions are very similar in terms of voltage profiles and cost minimization (Table 2, column 7), the former algorithm is much faster requiring on average about 50% less computing times.

6.5. Grid performance with low penetrations of PEVs

As utilization of electric vehicles has not been fully implemented in most countries, a more realistic scenario with more reasonable PEV penetrations of 3 and 5 percent has also been investigated. Simulation results are presented in Figs. 4 and 6 and Table 2, rows (5–6, 20–21). In addition, based on Figs. 4 and 6 it can be seen that without PEV charging coordination, the maximum power consumption increases from 0.84 MW (no PEV) to 0.86 MW (with 3% PEV penetration) and 0.87 MW (with 5% PEV penetration). Moreover, for 5% PEV penetration the maximum generation cost increases from 59$/MWh (no PEV charging) to 63$/MWh (uncoordinated PEV charging), while applying the proposed FDPSO limits the maximum generation cost level to 59$/MWh.

7. Conclusion

In a distribution system with high levels of PEV penetration, uncoordinated vehicle battery charging may impose substantial incremental loads to distribution transformers, cause voltage regulation problems, and considerably increase system losses and cost of generating energy. This paper proposes two optimal, fast and effective online PEV coordination strategy using FDPSO and FGA algorithms. Detailed simulations results for a 449-node SG network are presented and compared with uncoordinated and online coordinated PEV charging using MSS, DPSO, FDPSO, GA, FGA approaches. Main conclusions are:

- The proposed FDPSO approach is validated by comparing its solutions with DPSO, GA, FGA algorithms at different PEV penetration levels. It has superior performance and offers better solutions in terms of total daily generation cost compared to the uncoordinated as well as the other four coordinated strategies, by considering the impact of MEP, instantaneous DLC and the number of PEVs in the charging queue.
- FDPSO and FGA strategies result in similar solutions; however, the former approach based on DPSO is fundamentally faster (Table 2, column 7) and more suitable for online PEV coordination of large SG configurations.
- The FDPSO algorithms schedule the charging activities of randomly arriving PEVs at each timeslot based on smart meter information using online cost minimization while also taking advantage of the expert knowledge through fuzzy reasoning to postpone some vehicles charging such that the peak power consumption is shifted to the early morning hours to achieve further reductions in total costs and losses.
- Our future research will be on the consideration of practical issues and customer preferences such as requested plug-out times.

References

[1] Z. Luo, Z. Hu, Y. Song, Z. Xu, H. Lu, Optimal coordination of plug-in electric vehicles in power grids with cost-benefit analysis – Part I: enabling techniques, IEEE Trans. Power Syst. 28 (4) (2013) 3546–3555.
[2] P. Richardson, D. Flynn, A. Keane, Local versus centralized charging strategies for electric vehicles in low voltage distribution systems, IEEE Trans. Smart Grid 3 (2012) 1020–1028.
[3] K. Clement-Nyns, E. Haesen, J. Driesen, The impact of charging plug-in hybrid electric vehicles on a residential distribution grid, IEEE Trans. Power Syst. 25 (1) (2010) 371–380.
[4] W. Burke, D. Auslander, Residential electricity auction with uniform pricing and cost constraints, N. Am. Power Symp. (2009) 1–6.
[5] C.K. Wen, J.C. Chen, J.H. Teng, P. Ting, Decentralized plug-in electric vehicle charging selection algorithm in power systems, IEEE Trans. Smart Grid 3 (4) (2012) 1779–1789.
[6] M. Singh, I. Kar, P. Kumar, Influence of EV on grid power quality and optimizing the charging schedule to mitigate voltage imbalance and reduce power loss, in: Power Electronics and Motion Control Conference, 2010.
[7] K. Valentine, W.G. Temple, K.M. Zhang, Intelligent electric vehicle charging: rethinking the valley-fill, J. Power Sources 196 (24) (2011) 10717–10726.
[8] S.Y. Derakhshandeh, A.S. Masoum, S. Deilami, M.A.S. Masoum, M.E.H. Golshan, Coordination of generation scheduling with PEVs charging in industrial microgrids, IEEE Trans. Power Syst. 28 (3) (2013) 3451–3461.
[9] M.A.S. Masoum, P.S. Moses, S. Hajforoosh, Distribution transformer stress in smart grid with coordinated charging of plug-in electric vehicles, IEEE Power Energy Soc. Innov. Smart Grid (2012) 1–8.
[10] P. Richardson, D. Flynn, A. Keane, Optimal charging of electric vehicles in low-voltage distribution systems, IEEE Trans. Power Syst. 27 (1) (2012) 268–279.
[11] S. Deilami, A.S. Masoum, P.S. Moses, M.A.S. Masoum, Real-time coordination of plug-in electric vehicle charging in smart grids to minimize power losses and improve voltage profile, IEEE Trans. Smart Grid 2 (3) (2011) 456–467.
[12] A.S. Masoum, S. Deilami, P.S. Moses, M.A.S. Masoum, A. Abu-Siada, Smart load management of plug-in electric vehicles in distribution and residential networks with charging stations for peak shaving and loss minimization considering voltage regulation, IET Proc. Gener. Transm. Distrib. 5 (8) (2011) 877–888.
[13] A. Attanasio, G. Ghiani, L. Grandinetti, F. Guerriero, Auction algorithms for decentralized parallel machine scheduling, Parallel Comput. 32 (9) (2006) 701–709.
[14] R.A. Waraich, M.D. Galus, C. Dobler, M. Balmer, G. Andersson, K.W. Axhausen, Plug-in hybrid electric vehicles and smart grids: investigations based on a microsimulation, Transp. Res. C: Emerg. Technol. 28 (2013) 74–86.
[15] R. Liu, L. Dow, E. Liu, A survey of PEV impacts on electric utilities, in: IEEE PES ISGT Conference, 2011, pp. 1–8.
[16] T. Ma, O. Mohammed, Real-time plug-in electric vehicles charging control for V2G frequency regulation, in: 39th Annual IEEE Conference on Industrial Electronics Society (IECON), 2013, pp. 1197–1202.
[17] Y. Weifeng, Z. Junhua, W. Fushuan, A hierarchical decomposition approach for coordinated dispatch of plug-in electric vehicles, IEEE Trans. Power Syst. 28 (3) (2013).
[18] W. Di, C. Chengrui, D.C. Alprantis, Potential impacts of aggregator-controlled plug-in electric vehicles on distribution systems, in: IEEE International Conference on Computational Advances, 2011, pp. 105–108.
[19] W. Di, D.C. Alprantis, Y. Ling, Load scheduling and dispatch for aggregators of plug-in electric vehicles, IEEE Trans. Smart Grid 3 (1) (2012).
[20] C. Guille, G. Gross, A conceptual framework for the vehicle-to-grid (V2G) implementation, J. Energy Policy 37 (11) (2009).
[21] H.K. Nguyen, J.B. Song, Optimal charging and discharging for multiple PHEVs with demand side management in vehicle-to-building, IEEE J. Commun. Netw. 14 (6) (2012).
[22] C. Jin, J. Tang, P. Ghosh, Optimizing electric vehicle charging: a customer's perspective, IEEE Trans. Veh. Technol. (2013) 2919–2927.
[23] C.K. Nyns, E. Haesen, J. Driesen, The impact of charging plug-in hybrid electric vehicles on a residential distribution grid, IEEE Trans. Power Syst. (2010) 371–380.
[24] S.M.H. Nabavi, A. Kazemi, M.A.S. Masoum, Social welfare improvement by TCSC using real code based genetic algorithm in double-sided auction market, Adv. Electr. Comput. Eng. 11 (2) (2011) 99–106.
[25] J. Kennedy, R.C. Eberhart, A discrete binary version of particle swarm algorithm, in: IEEE International Conference on Computational Cybernetics and Simulation, vol. 5, 1997, pp. 4101–4108.
[26] S. Hajforoosh, S.M.H. Nabavi, M.A.S. Masoum, Coordinated aggregated-based particle swarm optimisation algorithm for congestion management in restructured power market by placement and sizing of unified power flow controller, IET Sci. Meas. Technol. 6 (4) (2012) 267–278.
[27] S.M.H. Nabavi, A. Kazemi, M.A.S. Masoum, Social welfare improvement by TCSC using real code based genetic algorithm in double-sided auction market, J. Sci. Iran. 19 (3) (2012).

[28] http://www.chargepoint.com/evs
[29] T.-K. Lee, Z. Baraket, T. Gordon, Z. Filipi, Stochastic modeling for studies of real-world PHEV usage: driving schedules and daily temporal distributions, IEEE Trans. Veh. Technol. 61 (4) (2012).
[30] A. Chakrabortty, M.D. Ilic, Control and Optimization Methods for Electric Smart Grids, vol. 3, 2012.
[31] M. LeMay, R. Nelli, G. Gross, C.A. Gunter, An integrated architecture for demand response communications and control, in: 41st Hawaii International Conference on System Sciences, 2008.
[32] A. Mishra, D. Irwin, P. Shenoy, T. Zhu, Scaling distributed energy storage for grid peak reduction, in: The Fourth International Conference on Future Energy Systems, 2013, pp. 3–14.
[33] M. Muratori, G. Rizzoni, Residential demand response: dynamic energy management and time-varying electricity pricing, IEEE Trans. Power Syst. (2015).
[34] M. Muratori, B.A.S. Leechb, G. Rizzoni, Role of residential demand response in modern electricity markets, J. Renew. Sustain. Energy Rev. 33 (2014) 546–553.